An exploratory model for predicting post-consumer recycled PET content in PET sheets

Dong Ho Kang [a], Rafael Auras [a,*], Keith Vorst [b], Jay Singh [b]

[a] School of Packaging, Michigan State University, East Lansing, MI 48824, USA
[b] Department of Industrial Technology and Packaging, California Polytechnic State University, San Luis Obispo, CA 93407, USA

An exploratory model for determining post-consumer recycled polyethylene terephthalate (PET) content in PET sheets for one specific stream of mechanically recycled PET (RPET) was developed. Six kinds of PET sheets with varying percent of virgin (V) and recycled (R) PET contents (i.e., 100V, 80V20R, 60V40R, 40V60R, 20V80R, and 100R PET) were commercially extruded. The optical, thermal, physicomechanical and barrier properties of the PET sheets were evaluated as function of RPET content. Differences were found between the sheets for UV and visible light absorption in the regions 200–350 nm and 670–700 nm, respectively. Intrinsic viscosities of 100V and 100R PET sheets were different. A censored normal multiple linear regression model including thermal, physical, optical and barrier properties was the best-fit model to predict VPET and RPET content in PET sheets.

1. Introduction

Polyethylene terephthalate (PET) consumption was approximately 15.3 million tons in 2009 [1]. In the U.S., the most widely used application for PET is the manufacture of bottles. Together with the increase of virgin (V) PET, the use of recycled post-consumer PET (RPET) flakes and resin for production of RPET products has continually increased. The main applications for RPET include fiber, beverage bottles, sheet and film, and non-food bottles. Total RPET resin converted to RPET products in the U.S. was estimated at 415 million kilograms in 2008, representing an increase of 21% since 1999 [2].

According to the Association of Postconsumer Plastic Recyclers (APR), approximately 95% of RPET is mechanically recycled in the U.S [2]. In general, mechanical recycling of RPET is performed by collecting scraps from homogeneous deposits like carbonated and non-carbonated drink bottles, and from heterogeneous deposits contaminated with polyvinyl chloride (PVC), nylon and various additives. One of the main drawbacks of RPET is the decrease in quality compared to virgin PET due to degradation caused by the simultaneous presence of retained moisture and contaminants during mechanical recycling [3]. The main degradation mechanisms of PET that occur during mechanical recycling are hydrolysis and thermal degradation. PET hydrolysis generally introduces carboxylic acid and hydroxyl-ester end groups. Thermal degradation generally produces carboxylic acid and vinyl ester end groups. These two degradation mechanisms reduce the molecular weight and decrease the intrinsic viscosity of the RPET [4]. Thus, RPET products generally present reduced optical, physical, mechanical and barrier properties [5–10].

Several studies have shown that increasing the percentage of RPET in PET products reduces their environmental footprint and provides cost advantages [11–13]. Thus, producers have incentives to make claims of higher RPET content in their products. Such claims require the ability to determine or estimate the amount of RPET. Attempts to develop techniques or models for determining the post-consumer recycled content of PET film, sheet and

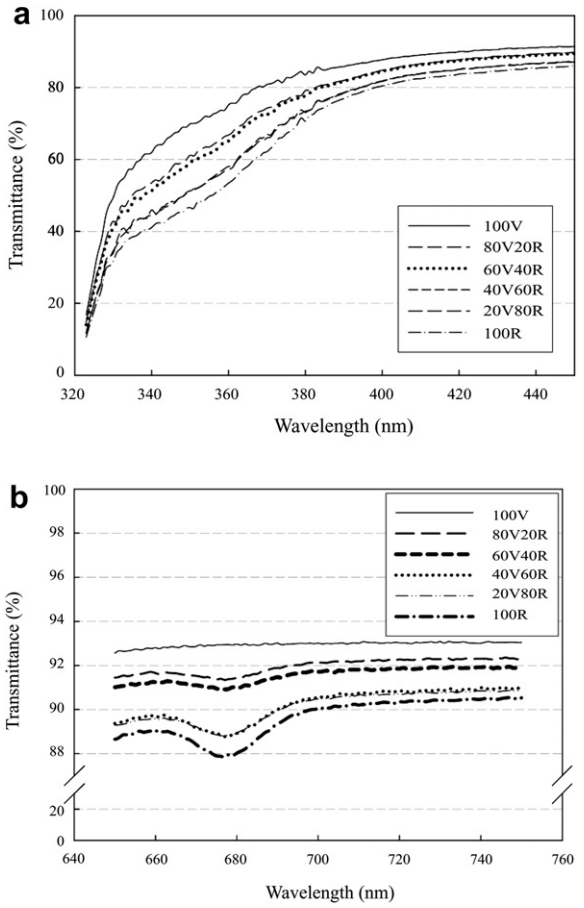

Fig. 1. a. Light transmission at 323–450 nm of PET sheets made from selected ratios of virgin (V) and recycled (R) PET. b. Light transmission at 650–750 nm of PET sheets made from selected ratios of virgin (V) and recycled (R) PET.

containers have been limited [14]. This is not surprising since the constituent units of RPET and PET are the same so that it is difficult to differentiate between the two materials with a single property determination. However, if solid state polycondensation is not done to obtain a higher grade RPET with higher intrinsic viscosity and weight average molecular weight, some property parameters could be used as indicators of RPET content, at least for the same specific stream of mechanically recycled PET.

The aim of this study was to develop an exploratory model, based on optical, thermal, physicomechanical and barrier properties, to quantify the amount of recycled PET, previously recovered by mechanical recycling, in PET/RPET sheets.

2. Methodology

2.1. Materials

Virgin PET resin, with an intrinsic viscosity of 0.80 ± 0.02 dl g^{-1}, was supplied by Eastman (Columbia, CA, USA). Recycled PET resin, derived mainly from recycling of bottles collected by the redeem bottle deposit system in California, was provided by ECO2 (Modesto, CA, USA).

2.2. RPET sheet production

Feedstocks of 100% VPET and 100% RPET were blended in six selected weight ratios from 0 to 100% RPET to produce sheets in a plant trial conducted at Peninsula Packaging Company (Exeter, CA, USA). The sheets were as follows: 100% VPET (100V), 80%VPET (80V20R), 60%VPET (60V40R), 40% VPET (40V60R), 20% VPET (20V80R) and 100% RPET (100R).

Virgin and recycled PET resins were initially stored in different silos and then mixed to produce the selected blends. Before mixing, the recycled PET resin was treated with a Conair model CGT 700 crystallizer (Franklin, PA, USA) for 45 min to 1 h to increase the crystalline areas of the resin; air flow temperature in the crystallizer was 155 °C (310 °F). A continuous gravimetric blending system (AEC Whitlock OS series blender, Wooddale, IL, USA) was used to mix RPET resin with VPET resin to achieve the desired compositions. The PET resin blends were subsequently dried with a Conair model CAG 2400 carousel drier (Franklin, PA, USA). After drying, the resin blends were fed to two single-screw Reifenhauser extruders (Troisdorf, Germany), extruded on one die and turned into sheets. The temperature profile was around 260 °C (500 °F) between the feed zone and the die.

2.3. UV-visible spectroscopy

UV-Visible spectroscopy was used to determine the light transmission of the six types of PET sheets. The UV-visible analyses were performed using a Perkin-Elmer

Table 1
Light transmission at different wavelengths for PET sheets made from selected ratios of virgin (V) and recycled (R) PET.

λ (nm)	Transmittance (%)					
	100V	80V20R	60V40R	40V60R	20V80R	100R
250	1.26 ± 0.57^{a}	1.51 ± 0.28^{a}	1.26 ± 0.33^{a}	1.57 ± 0.34^{a}	1.59 ± 0.37^{a}	1.10 ± 0.19^{a}
300	1.08 ± 0.37^{a}	1.23 ± 0.43^{a}	1.18 ± 0.33^{a}	1.20 ± 0.31^{a}	1.06 ± 0.24^{a}	1.39 ± 0.34^{a}
350	69.90 ± 1.60^{a}	61.18 ± 1.14^{b}	59.25 ± 0.57^{b}	54.07 ± 0.97^{c}	51.22 ± 0.94^{d}	46.62 ± 0.42^{e}
380	83.53 ± 0.81^{a}	79.18 ± 1.13^{b}	77.63 ± 0.75^{bc}	75.84 ± 1.29^{c}	73.43 ± 1.13^{d}	70.64 ± 0.76^{e}
676	92.93 ± 0.25^{a}	91.40 ± 0.46^{b}	90.93 ± 0.17^{b}	88.70 ± 0.26^{c}	88.82 ± 0.54^{c}	87.88 ± 0.12^{d}
677	92.94 ± 0.21^{a}	91.35 ± 0.41^{b}	90.92 ± 0.16^{b}	88.69 ± 0.24^{c}	88.81 ± 0.51^{c}	87.86 ± 0.12^{d}
678	92.94 ± 0.22^{a}	91.38 ± 0.42^{b}	90.94 ± 0.16^{b}	88.68 ± 0.24^{c}	88.85 ± 0.50^{c}	87.95 ± 0.12^{d}
700	93.01 ± 0.21^{a}	92.13 ± 0.40^{b}	91.72 ± 0.12^{b}	90.72 ± 0.25^{c}	90.48 ± 0.55^{c}	90.03 ± 0.12^{c}
800	93.01 ± 0.21^{a}	92.30 ± 0.35^{b}	92.00 ± 0.14^{b}	91.31 ± 0.22^{c}	90.94 ± 0.55^{c}	90.63 ± 0.15^{c}

Transmittance values are means ± standard deviation (SD); within each row, means with different superscripts are significantly different at $\alpha = 0.05$.

Table 2
Tristimulus color scale values and total color difference (ΔE) of selected PET sheets.

PET sheet type	L*	a^*	b^*	ΔE
100V	89.94 ± 0.022^{a}	-1.14 ± 0.015^{a}	1.10 ± 0.022^{a}	0.00 ± 0.00^{a}
80V20R	89.18 ± 0.110^{b}	-1.29 ± 0.013^{b}	1.62 ± 0.047^{b}	0.93 ± 0.08^{b}
60V40R	88.76 ± 0.283^{c}	-1.36 ± 0.019^{c}	1.55 ± 0.015^{b}	1.28 ± 0.26^{c}
40V60R	87.69 ± 0.103^{d}	-1.58 ± 0.017^{d}	2.31 ± 0.034^{c}	2.59 ± 0.09^{d}
20V80R	87.60 ± 0.168^{d}	-1.65 ± 0.012^{e}	2.39 ± 0.061^{d}	2.72 ± 0.16^{d}
100R	86.90 ± 0.075^{e}	-1.68 ± 0.005^{f}	3.10 ± 0.022^{e}	3.68 ± 0.06^{e}

Values are means ± SD; within the same column, means with different superscripts are significantly different at $\alpha = 0.05$.

Lambda 25 system (Waltham, MA, USA) with an integrating reflectance spectroscopy accessory (model RSA-E-20, Labsphere®, North Sulton, NH, USA); measurements were carried out at 480 nm/min and a wavelength range of 190–800 nm in transmittance (%) mode. All results are presented as transmittance values. At least five samples of each PET type were scanned.

2.4. Color measurement

Tristimulus colorimetry of PET sheet samples was carried out using a HunterLab LabScan XE (Reston, VA, USA) colorimeter, and measurements were converted by the instrument to L*a*b* color scale values. The control sample was the 100% VPET sheet. Differences in L*, a*, and b* values between the control and other sheets was expressed as ΔL^*, Δa^*, and Δb^*. For each sheet type, five samples were measured and color values were averaged before calculating total color difference (ΔE) values by Eq.(1) [15].

$$\Delta E = \sqrt{\Delta L^2 + \Delta a^2 + \Delta b^2} \tag{1}$$

2.5. Differential scanning calorimetry

A TA Instruments DSC-Q100 differential scanning calorimeter (New Castle, DE, USA) was used to determine the thermal properties of the PET sheets. Each sample (12–15 g) was tested under a heat/cool/heat cycle between 40 and 300 °C at a rate of 10 °C per min in a nitrogen atmosphere. The glass transition temperature (T_g), onset of cold crystallization temperature ($T_{cc\ onset}$), cold crystallization temperature (T_{cc}), onset of melting temperature ($T_{m\ onset}$) and melting temperature (T_m) of the samples were recorded. $T_{cc\ onset}$ and T_{cc} values were obtained from the first heating run, and T_g, $T_{m\ onset}$ and T_m from the second heating run. The degree of crystallinity, χ_c, for the samples was calculated as follows:

$$\chi_c(wt.\%) = 100 \times \frac{\Delta H_m - \Delta H_c}{\Delta H_m^\circ} \tag{2}$$

where ΔH_m is the heat of melting, ΔH_c is the heat of crystallization, ΔH_m° is the heat of fusion of 100% crystalline PET ($\Delta H_m^\circ = 140$ J/g) [16].

2.6. Measurement of barrier properties

The water vapor transmission rate (WVTR) was measured with a Permatran™ C3/31 system (Modern Controls Inc., Minneapolis, MN,) according to ASTM F1249 [17]. The testing conditions were 37.8 ± 0.5 °C at ~100% relative humidity (RH). All measurements were performed in triplicate for each sheet type. The WVTR values were used to calculate the water vapor permeability (WVP) value:

$$\textit{Water vapor permeability} = \frac{\textit{Water vapor transmission rate}\ (kg) \times \textit{thickness}\ (m)}{\textit{partial pressure}\ \left(Pa\right) \times \textit{time}\ \left(s\right) \times \textit{area}\ (m^2)} \tag{3}$$

The oxygen transmission rate (OTR) was measured using an Illinois 8001 oxygen permeation analyzer (Illinois Instruments Inc., Johnsburg, IL, USA). The test was performed in accordance with ASTM D 3985 [18] at 23 ± 0.5 °C and 50 ± 2% RH. All measurements were performed in triplicate for each PET sheet type. OTR values were used to calculate the oxygen permeability (OP) value:

$$\textit{Oxygen permeability} = \frac{\textit{Oxygen transmission rate}\ (kg) \times \textit{thickness}\ (m)}{\textit{partial pressure}\ \left(Pa\right) \times \textit{time}\ \left(s\right) \times \textit{area}\ (m^2)} \tag{4}$$

2.7. ^1H nuclear magnetic resonance (NMR) spectroscopy

^1H NMR spectra were obtained on a Varian VXR-500 FT spectrometer. ^1H spectra were observed at 500 MHz. To

Table 3
Thermal properties of selected PET sheets.

PET sheet type	T_g (°C)	T_{cc} (°C)	T_c (°C)	T_m (°C)	χ_c (wt. %)
100V	79.2 ± 0.2^{a}	137.0 ± 0.5^{a}	168.9 ± 1.8^{a}	245.2 ± 0.1^{a}	6.9 ± 0.9^{a}
80V20R	77.1 ± 0.4^{b}	134.4 ± 0.2^{b}	184.6 ± 0.7^{b}	245.6 ± 0.4^{a}	8.6 ± 1.5^{ab}
60V40R	77.7 ± 0.4^{b}	133.3 ± 0.4^{bd}	185.1 ± 0.6^{bc}	245.8 ± 0.4^{ab}	9.3 ± 0.5^{ab}
40V60R	77.2 ± 0.4^{b}	130.6 ± 0.8^{c}	189.8 ± 2.4^{c}	246.7 ± 0.7^{bc}	10.1 ± 0.9^{b}
20V80R	77.9 ± 0.5^{b}	132.1 ± 0.6^{d}	188.6 ± 0.3^{c}	247.0 ± 0.2^{c}	9.3 ± 1.6^{ab}
100R	77.5 ± 0.5^{b}	132.5 ± 0.2^{d}	190.9 ± 0.9^{c}	247.5 ± 0.1^{c}	8.1 ± 0.7^{ab}

Values are means ± SD; within the same column, means with different superscripts are significantly different at $\alpha = 0.05$.

Table 4
Water vapor and oxygen permeabilities of selected PET sheets.

PET sheet type	Water vapor permeability ($kg \times m/m^2 \times Pa \times sec$) ($\times 10^{-15}$)	Oxygen permeability ($kg \times m/m^2 \times Pa \times sec$) ($\times 10^{-19}$)
100V	2.73 ± 0.08^{ad}	5.86 ± 0.13^{a}
80V20R	2.52 ± 0.03^{b}	5.62 ± 0.06^{ab}
60V40R	2.58 ± 0.09^{b}	5.26 ± 0.08^{c}
40V60R	2.65 ± 0.05^{c}	5.34 ± 0.24^{bc}
20V80R	2.72 ± 0.02^{ac}	5.32 ± 0.06^{bc}
100R	2.76 ± 0.02^{d}	5.54 ± 0.15^{bc}

Values are means ± SD; within the same column, means with different superscripts are significantly different at $\alpha = 0.05$.

prepare samples for analysis, the PET sheets were dissolved in a 2 to 1 (vol/vol) mixture of trifluoroacetic acid/chloroform. This mixture dissolves the high molecular weight polyesters to analyze the end group signal at ambient temperature [19]. Chemical shifts were reported in parts per million from tetramethylsilane. Samples were tested in triplicate.

2.8. Viscosimetry

Solution viscosity was measured using a 1C Ubbelhode capillary viscometer (approximated constant: 0.03 mm^2/s^2, kinematic viscosity range: 6–30 mm^2/s). PET solutions were obtained by dissolving the selected sheets in a 60:40 mixture (by volume) of phenol and 1, 1, 2, 2-tetrachloroethane (Sigma–Aldrich, St. Louis, MO) at 24 ± 0.5 °C. In order to measure the intrinsic viscosity and viscosity average molecular weight, 4 different ratios of solutions were prepared and measured. Viscosity measurements were performed in accordance with ASTM D445 and D446 [20,21]. The intrinsic viscosity, η, was determined by the Huggins equation, Eq. (5). The viscosity average molecular weight, $\overline{M}_v$, was determined by the Mark–Houwink relationship, Eq. (6), where $K = 7.44 \times 10^{-4}$ dl g^{-1} and $\alpha = 0.648$ at 25 °C [22].

$$\frac{\eta_{sp}}{c} = [\eta] + k'[\eta]^2 c \tag{5}$$

$$[\eta] = K \times M_v^{\alpha} \tag{6}$$

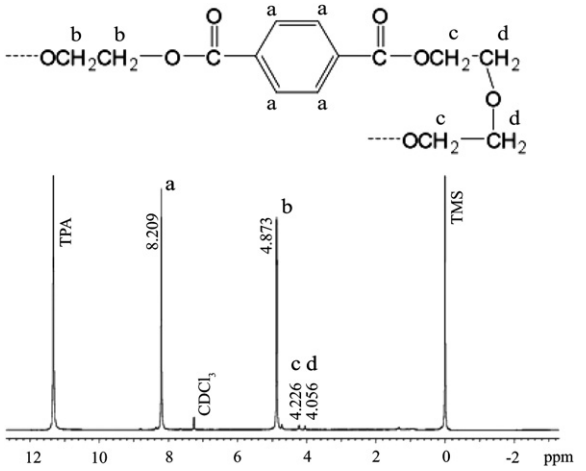

Fig. 2. ^{1}H NMR spectrum of 100V PET sample in TFA/$CDCl_3$.

2.9. Statistical analysis and determination of a prediction model

The optical, physicomechanical, thermal, and barrier properties of PET sheets with various recycled and virgin PET contents were used to create a multiple linear prediction model. One-way ANOVA and Tukey's HSD (Honestly Significant Differences) test were performed to conduct multiple comparisons of each experimental data set ($\alpha = 0.05$). SAS 2004 software (SAS Institute Inc., Cary, NC, USA) was used to conduct the statistics and the prediction model selection.

Multiple linear regression was performed to find the linear model that best predicts the percent of virgin or recycled PET in the sheets. Sixteen independent variables were selected from the different experiments. Since 2^{16} possible subset models could be produced, a model selection procedure was conducted using the Akaike's second order information criterion method, determined by Eq. (7), to evaluate all possible subsets of multiple regression models to determine the best model for up to 10 independent variables [23]. The model with the smallest AIC_c was considered to be the best fitting model. The AIC_c was used because it performs better than AIC when sample size is small relative to the number of parameters [25].

$$AIC_c = AIC + \frac{2 \times K \times (K+1)}{(n-K-1)} \tag{7}$$

where K is the number of parameters in the fitted model and n is the number of observations. Specifically, in order to address uncertainty of model selection, every model was ranked from lowest AIC to highest. The model with the lowest AIC score was used to determine the AIC_c score (calculated from AIC score in PROC REG, SAS 2004). Each independent variable observation was centered to stabilize variation as indicated in Eq. (8) [24].

$$x_i^{**} = \frac{(x_i - Midpoint\ (x))}{Half\ Range\ (x)} \tag{8}$$

Although many models for predicting VPET and RPET content in PET sheets were obtained, a successful model was limited to having a minimum of independent variables without compromising the decrease of the AIC_c score. This is often known as the principle of Occam's Razor or the Principle of Parsimony [24]. To evaluate the degree of multicolinearity within the independent variables, the condition index was used (COLLIN option in PROC REG, SAS 2004). From the best-fitted model, additional scenarios were conducted with a censored normal multiple linear regression model or Tobit model. By using Tobit analysis, the dependent variable has a number of its values clustered at a limiting value, such as 0 and 1 [26]. In this study, this adjustment was applied to control the boundary conditions of VPET within 0 and 100%. Model validation was performed by re-measuring the properties mentioned above for the 6 types of PET sheets in triplicate and calculating the percentage of absolute error and squared error:

$$Absolute\ error = 1 - \frac{\sum |Y - \widehat{Y}|}{\sum |Y - \overline{Y}|} \tag{9}$$

Table 5
Composition ratio of selected PET sheets for aromatic protons (a), ethylene glycol protons (b), and diethylene glycol protons (c, d).

PET sheet type	Composition ratio (mol ratio)				
	a	b	c	d	c + d
100V	1	1.031 ± 0.003^{ab}	0.036 ± 0.002^{a}	0.019 ± 0.001^{a}	0.055 ± 0.002^{a}
80V20R	1	1.037 ± 0.004^{c}	0.039 ± 0.002^{a}	0.021 ± 0.002^{abc}	0.060 ± 0.004^{abc}
60V40R	1	1.036 ± 0.000^{bc}	0.035 ± 0.007^{a}	0.022 ± 0.000^{bc}	0.057 ± 0.006^{bc}
40V60R	1	1.032 ± 0.002^{abc}	0.042 ± 0.001^{a}	0.022 ± 0.001^{bc}	0.064 ± 0.002^{bc}
20V80R	1	1.036 ± 0.002^{bc}	0.041 ± 0.001^{a}	0.023 ± 0.001^{c}	0.064 ± 0.002^{c}
100R	1	1.029 ± 0.000^{a}	0.037 ± 0.001^{a}	0.019 ± 0.001^{ab}	0.057 ± 0.001^{ab}

Values are means ± SD; within the same column, means with different superscripts are significantly different at $\alpha = 0.05$.

$$Squared\ error = 1 - \frac{\sum\left(Y - \widehat{Y}\right)^2}{\sum(Y - \overline{Y})^2} \quad (10)$$

where Y is the value of the response variable, $\widehat{Y}$ is the predicted value based on the model-building data set, and $\overline{Y}$ is the mean of the response variable in the validation data set. In general, both absolute and squared errors are used for estimating the predictive accuracy of a model.

3. Results and discussion

3.1. Optical properties

UV-visible light transmission: The chromophorie groups in PET are the benzene ring, which absorbs in the UV region at 198 and 255 nm maximum wavelengths, and the ester group (-COOR), which absorbs at the 205 nm wavelength through $\pi \rightarrow \pi^*$ transition and $\eta \rightarrow \pi^*$ transition [27,28]. Therefore, the absorbance of PET mainly occurred in the UV region (190–400 nm), primarily between 330 and 390 nm (Fig. 1a). Fig. 1b shows another absorbance peak between 675 and 678 nm for some PET sheets, which corresponds to the red light region. This absorbance may be due to residual contaminants in the RPET component of the sheets, especially fragments of green or blue colored bottles and printed ink labels.

Table 1 provides the light transmission values at 350, 380, 676, 677 and 678 nm for the PET sheets containing selected amounts of RPET, which had statistically significant differences ($\alpha = 0.05$). At each of these wavelengths, % transmission of the sheets decreased as RPET content increased.

Color: Results of color measurement as expressed in the L* a* b* scale for the various PET sheets are shown in Table 2. In sheets with greater RPET content, the color was darker or more gray (L* values decreased), more green (a* values were more negative), and more yellow (b* values were more positive). RPET flakes may contain fragments of green or blue colored bottles, so incorporation of this resin in PET sheets would result in decreased (more negative) a* values. In general, PET yellowing is associated with thermal degradation [29]. During PET processing above its melting temperature, the thermal cleavage of the PET ester bond results in shorter chains with acid and vinyl ester end group formation [4]. The carboxyl end group content generated by PET processing promotes oxidation of PET [30]. Therefore, repeated recycling generates more carboxyl end groups in PET, and causes more oxidation. Therefore, greater content of RPET in the sheets leads to increased b* values.

Table 6
Intrinsic viscosity, η, and viscosity molecular weight, $\overline{M}_V$, of solutions of selected PET sheets at 24 ± 0.5 °C.

PET sheet type	η (dl/g)	$\overline{M}_V$ (g/mol)
100V	0.722 ± 0.029^{a}	40742 ± 2052^{a}
80V20R	0.696 ± 0.022^{a}	38449 ± 1839^{a}
60V40R	0.630 ± 0.006^{b}	32989 ± 449^{b}
40V60R	0.631 ± 0.006^{b}	33038 ± 478^{b}
20V80R	0.607 ± 0.009^{b}	31141 ± 695^{b}
100R	0.533 ± 0.017^{c}	25479 ± 1275^{c}

Values are means ± SD; within the same column, means with different superscripts are significantly different at $\alpha = 0.05$.

3.2. Thermal properties

Table 3 shows the thermal properties, i.e., T_g, T_{cc}, T_c, T_m, and χ_c, obtained for the selected PET sheets. For T_g, only 100V shows significant difference so it is not a good indicator for amount of recycled PET. Cold crystallization and crystallization temperature shows statistically significant differences between the six type of sheet, but there was not a linear trend with recycled PET content. Higher impurity amounts in 100 RPET delayed the crystallization rate, hence

Table 7
Independent variables used as indicators for RPET content in model selection.

Category	Independent variable	Model notation
Differential scanning calorimetry	Glass transition temperature	TG
	Cold crystallization temperature	TCC
	Crystallization temperature	TC
	Melting temperature	TM
	% Crystalline area	DH
UV–visible spectroscopy	350 nm	UV350
	380 nm	UV380
	675 nm	UV675
Viscosimetry	Intrinsic viscosity	IV
	Viscosity molecular weight	VM
Barrier	Water vapor permeability	WVP
	Oxygen permeability	OP
Nuclear magnetic resonance	Sum of mol ratio of diethylene glycol	NMR424
Colorimetry	L*	L
	a*	a
	b*	b

Table 8
The seven models with the lower *AIC* and AIC_c scores.

AIC	AIC_c	Independent variables in the model
−131.5757	−115.5757	TC, TM, UV350, UV380, UV675, VM, WVP, a
−131.6640	−109.1640	TC, TM, DH, UV350, UV380, UV675, IV, WVP, a
−131.3784	−115.3784	TC, TM, UV350, UV380, UV675, IV, WVP, a
−131.4491	−108.9491	TC, TM, DH, UV350, UV380, UV675, VM, WVP, a
−131.0603	−115.0603	TG, TCC, DH, UV350, UV380, UV675, L, a
−131.3392	−99.9106	TC, TM, DH, UV350, UV380, UV675, VM, WVP, a, b
−131.2582	−99.8296	TC, TM, DH, UV350, UV380, UV675, IV, WVP, a, b

The shadowed row indicates the *AIC* and AIC_c values and the independent variables for the final selected model in this study.

Table 9
Parameter estimates for the multiple linear regression and Tobit models.

Independent variable and (constant)	Multiple linear regression model		Tobit model	
	Parameter estimate	*P* value	Parameter estimate	*P* value
Intercept	0.563 ± 0.015	<0.0001	0.545 ± 0.011	<0.0001
TC (a)	0.167 ± 0.037	0.0015	0.097 ± 0.037	0.0094
TM (b)	−0.052 ± 0.026	0.0716	−0.037 ± 0.017	0.0313
UV350 (c)	0.306 ± 0.068	0.0015	0.360 ± 0.063	<0.0001
UV380 (d)	0.158 ± 0.060	0.0273	0.140 ± 0.041	0.0007
UV676 (e)	−0.146 ± 0.042	0.0071	−0.158 ± 0.027	<0.0001
VM (f)	0.089 ± 0.030	0.0154	0.116 ± 0.023	<0.0001
WVP (g)	0.035 ± 0.019	0.1063	0.014 ± 0.014	0.3327
a (h)	0.254 ± 0.046	0.0004	0.206 ± 0.035	<0.0001
Sigma*	N/A	N/A	0.013 ± 0.003	<0.0001

N/A: not applicable.
*Sigma corresponds to the estimate of the error variance σ.

Table 10
Remeasured data obtained for the 8 independent variables for model validation.

	PET sheet type					
	100V	80V20R	60V40R	40V60R	20V80R	100R
TC	170.09 ± 1.50^{a}	184.18 ± 0.72^{b}	185.56 ± 1.10^{b}	188.66 ± 0.42^{c}	190.76 ± 1.0^{cd}	192.76 ± 1.10^{d}
TM	245.66 ± 0.14^{a}	245.55 ± 0.08^{a}	245.55 ± 0.03^{a}	246.46 ± 0.04^{b}	247.05 ± 0.15^{c}	247.75 ± 0.02^{d}
DH	34.73 ± 7.74^{a}	38.49 ± 1.22^{a}	40.06 ± 1.21^{a}	40.70 ± 0.55^{a}	39.86 ± 0.85^{a}	41.36 ± 2.05^{a}
UV350	69.66 ± 0.86^{a}	63.23 ± 2.00^{b}	59.14 ± 0.25^{c}	56.18 ± 0.65^{d}	54.03 ± 1.20^{d}	45.79 ± 0.23^{e}
UV380	80.88 ± 1.9^{ab}	82.78 ± 2.40^{b}	75.39 ± 1.20^{ac}	74.44 ± 1.70^{c}	76.89 ± 3.20^{abc}	71.48 ± 2.00^{c}
UV676	92.49 ± 0.22^{a}	91.42 ± 0.10^{ab}	90.52 ± 0.91^{b}	88.43 ± 0.06^{cd}	89.30 ± 0.30^{c}	87.93 ± 0.10^{d}
IV	0.724 ± 0.005^{a}	0.709 ± 0.001^{a}	0.633 ± 0.008^{b}	0.633 ± 0.015^{b}	0.607 ± 0.009^{c}	0.546 ± 0.003^{d}
VM	40887 ± 402^{a}	39561 ± 84^{a}	33193 ± 680^{b}	33210 ± 1250^{b}	31109 ± 696^{c}	26457 ± 217^{d}
WVP (10^{-15})	2.865 ± 0.09^{a}	2.828 ± 0.05^{a}	2.841 ± 0.110^{a}	2.744 ± 0.140^{a}	2.776 ± 0.130^{a}	2.679 ± 0.060^{a}
a	-1.04 ± 0.00^{a}	-1.26 ± 0.01^{a}	-1.28 ± 0.01^{a}	-1.45 ± 0.01^{a}	-1.58 ± 0.01^{a}	-1.66 ± 0.02^{a}

Values are means ± SD; within the same row, means with different superscripts are significantly different at $\alpha = 0.05$.

increasing T_c. Moreover, the presence of impurities at just 20%wt. reduces T_g.

3.3. Barrier properties

Table 4 shows that statistically significant differences ($\alpha = 0.05$) were found between the WVP and OP values for the selected PET sheets, but there was no clear relationship between permeability and increased RPET content. Variation of 10% in barrier properties is not uncommon due to processing and final polymer morphology.

3.4. Physicochemical properties

^{1}H NMR spectra: Since recycled PET resin in this work was processed through mechanical recycling, the degradation reactions occurring are hydrolysis and thermal degradation. Thus, more diethylene glycol derived from carboxylic acid, hydroxyl-ester and vinyl ester end groups was found with increasing RPET content in PET sheets.

Fig. 2 illustrates an example of one ^{1}H NMR spectrum obtained for 100V PET sample. Four peaks were attributed to four kinds of ^{1}H protons. The most obvious peak is a singlet at δ 8.2 ppm arising from aromatic protons (a) of the PET repeat units. A mixture of TFA/$CDCl_3$ (2:1) was used as the solvent for the PET samples; trifluoroacetic acid anhydride leads to a rapid esterification of the OH end-groups. As a consequence, the two CH_2 signals of the ethylene glycol end-groups (b) shifted down field and coalesced with the main signal at δ 4.8 ppm [31]. The diethylene glycol (c, d) signals remained unchanged. The small peaks between δ 1 and 2 ppm were identified as impurities of $CDCl_3$ and residuals of moisture, respectively [31].

Table 5 indicates the composition ratios of aromatic protons (a), ethylene glycol protons (b), and diethylene glycol protons (c, d) in the selected PET sheets. Protons of

Table 11
Comparison of actual virgin PET content and predicted virgin PET content according to the selected model analyzed by multiple linear regression and Tobit models.

Actual virgin PET content in PET sheets (%)	Predicted virgin PET content (%)	
	Regression model	Tobit model
100	94.53 ± 0.04	99.05 ± 0.02
80	88.36 ± 0.03	87.42 ± 0.03
60	60.75 ± 0.06	57.43 ± 0.06
40	48.80 ± 0.04	48.65 ± 0.03
20	31.38 ± 0.09	29.79 ± 0.08
0	−6.26 ± 0.08	0 ± 0
Absolute error	0.75	0.82
Squared error	0.94	0.97

Selected model is composed of TC, TM, UV350, UV380, UV676, VM, WVTR and *a*.

ethylene glycol and diethylene glycol were considered as recycling indicators for the differences found between PET sheets containing various percentages of virgin and recycled PET. Protons of end groups in 60V40R, 40V60R and 20V80R PET were statistically significantly higher than in 100V PET.

Intrinsic viscosity: Table 6 indicates the intrinsic viscosity, η, and viscosity average molecular weight, $\overline{M}_V$, for PET solutions containing different RPET contents at 24 ± 0.5 °C. All samples had intrinsic viscosity values between 0.53 and 0.72 dl/g; viscosity molecular weights ranged from 25,000 to 41,000 g/mol. Statistically significant differences in η was found between some PET sheet types, particularly between 100V and 100R PET. In general, the higher the percent of RPET in the PET sheet solution, the lower the corresponding η and $\overline{M}_V$. This reduction in η may be due to contaminants in recycled PET, such as retained moisture and adhesives [32], which generate acid compounds during processing and catalyze the hydrolytic cleavage of the ester bond to yield carboxylic acid and hydroxyl-ester end groups, thus reducing the polymer chains and lowering η and $\overline{M}_V$[22]. Also, the additional heat history of RPET may play a role in reducing η.

3.5. Model selection

The 16 independent variables selected in this study to be used as indicators for RPET content are shown in Table 7. These variables all showed statistically significant changes in PET sheets made with various ratios of VPET and RPET.

A total of 2^{16} subset models were produced, and seven full models have the lower AIC_c values (Table 8). A model with 8 independent variables and the lowest AIC_c value was selected and is described by Eq. (11):

$$VPET\% = Intercept + a \times TC + b \times TM + c \times UV350 + d \times UV380 + e \times UV675 + f \times VM + g \times WVP + h \times a^{*} + \varepsilon \quad (11)$$

where TC is crystallization temperature, TM is melting temperature, UV350 is light transmission value at 350 nm, UV380 is light transmission value at 380 nm, UV675 is light transmission value at 675, VM is viscosity molecular weight, WVP is water vapor permeability, a^* is color value of a* and ε is the residual error. In Eq. (11), the values 'a, b, c, d, e, f, g, and h' are the fitting constants of the regression model.

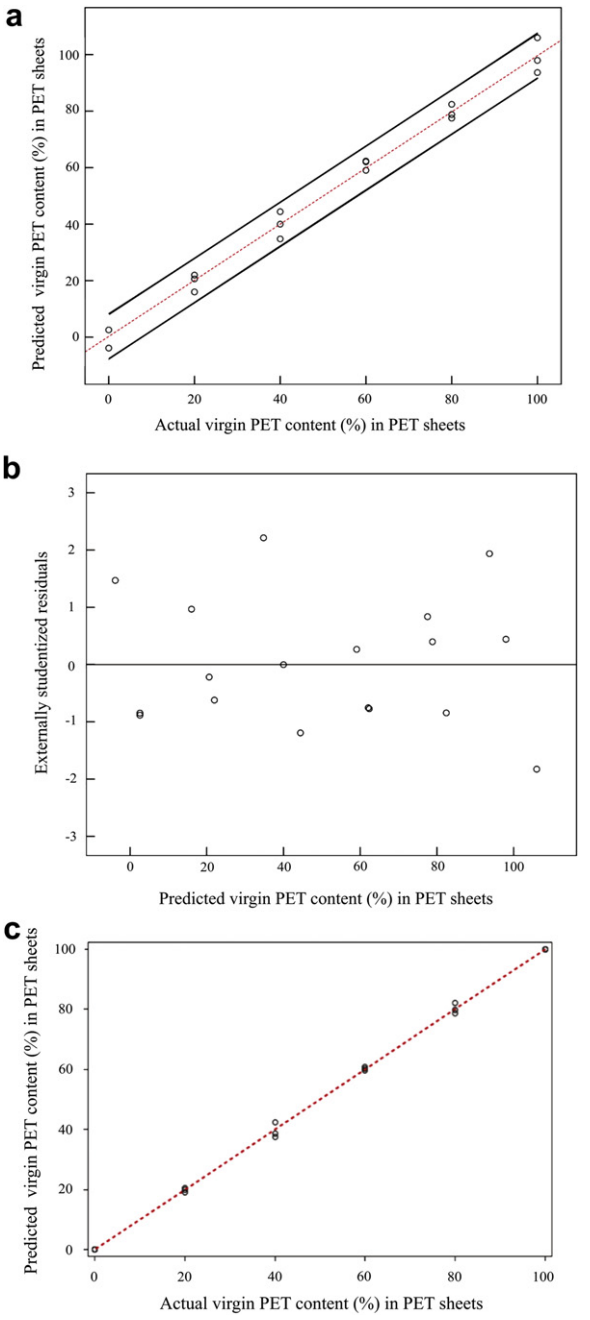

Fig. 3. a. Predicted content of virgin PET in the PET sheets (as determined by the selected multiple linear regression model) expressed as a function of the actual content of virgin PET. Note: outer lines represent 95% confidence intervals. b. Externally studentized residuals for the selected multiple linear regression model vs predictions of virgin PET content in the PET sheets. c. Predicted content of virgin PET in the PET sheets (as determined by the Tobit model) vs the actual virgin PET content.

Table 12
Parameter estimates for the reduced multiple linear regression and reduced Tobit models.

Independent variable and (constant)	Reduced regression model		Reduced Tobit model	
	Parameter estimate	*P* value	Parameter estimate	*P* value
Intercept	0.523 ± 0.021	<0.0001	0.499 ± 0.021	<0.0001
UV350	0.213 ± 0.104	0.0589	0.500 ± 0.129	0.0001
VM (f)	0.163 ± 0.053	0.0084	0.171 ± 0.050	0.0007
a (h)	0.189 ± 0.076	0.0257	0.029 ± 0.080	0.7144
Sigma	N/A	N/A	0.033 ± 0.007	<0.0001

N/A: not applicable.
Sigma corresponds to the estimate of the error variance σ.

A multiple linear regression and a censored normal multiple regression model (Tobit model) were fitted to Eq. (11). Equation parameters of both analyses assigned for each independent variable are listed in Table 9.

To evaluate the degree of multicolinearity between each of the independent variables, the condition index was used. For our 8 independent variables, the maximum value for the condition index was 24.9. An informal rule of thumb is that if the condition number is lower than 30, multicolinearity is not a serious concern [33].

3.6. Model validation

The 8 independent variables were re-measured using new additional sampled PET sheets to validate the multiple linear regression and Tobit models; the data obtained are provided in Table 10.

Since the data set used for establishing this model is centered to stabilize variation, re-measured data were rescaled to run. Table 11 shows the predicted VPET percentage for the model variables, as determined with and without the Tobit adjustment in Table 7. According to the absolute (0.75 and 0.82) and squared error (0.94 and 0.97) stated in Table 11, the Tobit model shows better predictive accuracy than the multiple linear regression model.Since the Tobit model used censored normal distribution of the VPET between 0 and 100%, the final squared error is minimized.

The regression and Tobit models of the predicted virgin PET contents of the PET sheets are illustrated in Fig. 3a–c. Fig. 3a shows that the predicted values of virgin PET content in PET sheets are linearly aligned as a function of the actual virgin PET content. All actual values lay within the 95% confidence band. Fig. 3b shows the externally studentized residuals for the multiple linear regression analysis; no normality and outlier problems were apparent for this model. Finally, Fig. 3c shows the actual percentage of virgin PET content in the PET sheets as a function of the predicted percentage of virgin PET for the Tobit model.

One limitation of the two models that should be considered is that they were developed considering a single mechanically-recycled PET stream (provided by ECO2, California, as described earlier). Therefore, further validation is needed to apply these models to other recycled PET streams and products.

Since the measurement of 8 independent variables may be cost prohibitive for everyday industrial applications, a reduced model for predicting RPET content is presented in Table 12. The reduced model considers just 3 of the independent variables: intrinsic viscosity (VM), *a**, and UV350. Although the full (original) Tobit model (with an absolute error of 0.82 and a squared error of 0 97) is preferred, the reduced Tobit model, which has an absolute error of 0.86 and a squared error of 0.98 (Table 13), could be used to obtain more rapid results. Also, in the reduced model, the *AIC* and AIC_c values, which are much more robust indicators of goodness of fit of the data, were −105.969 and −104.255, respectively; these values are higher than those obtained for the full multiple linear regression and Tobit models. Therefore, these higher *AIC* and AIC_c values indicate that, whenever possible, the full model should be used for prediction. The same constraints applied to the full model must be considered when using the reduced model. Although these models may not be directly applied to other recycling streams, the methodology and parameters used to predict the recycled and virgin PET content in PET sheets in this study may well translate to other scenarios, and they can be used as a starting point for prediction purposes under similar boundary conditions.

Table 13
Comparison of actual virgin PET content and predicted virgin PET content according to the reduced model analyzed by multiple linear regression and Tobit models.

Actual virgin PET content in PET sheets (%)	Predicted virgin PET content (%)	
	Reduced regression model	Reduced Tobit model
100	109.49 ± 0.01	100 ± 0.00
80	82.56 ± 0.04	87.98 ± 0.08
60	59.85 ± 0.01	56.45 ± 0.02
40	45.02 ± 0.03	43.13 ± 0.05
20	29.28 ± 0.03	28.76 ± 0.06
0	0.96 ± 0.02	0.00 ± 0.00
Absolute error	0.84	0.86
Squared error	0.97	0.98

Reduced model is composed of UV350, VM, and *a*.

4. Conclusion

Properties of PET sheets with varying percent of virgin and recycled PET were analyzed to establish an exploratory model to predict VPET and RPET contents in PET sheets using the first and second order Akaike's information criteria (AIC & AIC_c). Specifically, visible absorption arising around 678 nm was attributed to fragments of green or blue colored bottles and printed ink labels. It was found that higher RPET content increases grey, green and yellow color measurements. Reduction of intrinsic viscosity was found as recycled PET content increased. A good prediction model for recycled and virgin PET was found for a censored normal multiple linear regression model composed of 8 independent variables, crystallization and melting temperatures, UV-visible spectroscopy at 350, 380 and 675 nm, intrinsic viscosity, water vapor permeability and the a^* value from the CIELAB color system. A reduced model including UV-visible spectroscopy at 350, intrinsic viscosity, and a^* value is also presented for practical applications. These models are only applicable to the specific mechanical RPET stream and one VPET stream for which they were developed.

Acknowledgments

The Peninsula Packaging Company (Exeter, CA, USA) is acknowledged for providing the PET sheets for this project. The authors thank Daniel Johns (Chemistry Department, MSU) for help with interpreting the nuclear magnetic resonance study, and Wei Wang for support with the statistical analysis. The authors also thank Susan E. M. Selke and Satish Joshi (SoP, MSU) and Roland Geyer and Brandon Kuczenski (Environmental Science and Management, University of California) for fruitful discussions about recycled PET. This project was partially funded by the California Department of Resources Recycling and Recovery (Grant #5007-503).

References

[1] The polyethylene terephthalate (PET) market to 2020-carbonated soft drinks and bottled water market. GBI Research, 2010.
[2] National Association for PET, Container Resources, 2008 Report on Post Consumer PET Container Recycling Activity (2009) Sonoma, California 95476.
[3] G. Karayannidis, E. Psalida, Chain extension of recycled poly (ethylene terephthalate) with 2, 2'-(1, 4-phenylene) bis (2-oxazoline), J. Appl. Polym. Sci. 77 (10) (2000) 2206–2211.
[4] N. Cardi, R. Po, G. Giannotta, Chain extension of recycled poly (ethylene terephthalate) with 2, 2'-bis (2-oxazoline), J. Appl. Polym. Sci. 50 (9) (1993) 1501–1509.
[5] M. Paci, F. La Mantia, Competition between degradation and chain extension during processing of reclaimed poly (ethylene terephthalate), Polym. Degrad. Stabil. 61 (3) (1998) 417–420.
[6] A. Pawlak, M. Pluta, J. Morawiec, A. Galeski, M. Pracella, Characterization of scrap poly (ethylene terephthalate), Eur. Polym. J. 36 (9) (2000) 1875–1884.
[7] F. Villain, J. Coudane, M. Vert, Thermal degradation of polyethylene terephthalate: study of polymer stabilization, Polym. Degrad. Stabil. 49 (3) (1995) 393–398.
[8] A. Oromiehie, A. Mamizadeh, Recycling PET beverage bottles and improving properties, Polym. Int. 53 (6) (2004) 728–732.
[9] F. Awaja, D. Pavel, Recycling of PET, Eur. Polym. J. 41 (7) (2005) 1453–1477.
[10] M. Paci, F. La Mantia, Influence of small amounts of polyvinylchloride on the recycling of polyethylene terephthalate, Polym. Degrad. Stabil. 63 (1) (1999) 11–14.
[11] S. Madival, R. Auras, P. Singh, R. Narayan, Assessment of the environmental profile of PLA, PET and PS clamshell containers using LCA methodology, J. Clean Prod. 17 (13) (2009) 1183–1194.
[12] U. Arena, M.L. Mastellone, F. Perugini, Life cycle assessment of a plastic packaging recycling system, Int. J. LCA 8 (2) (2003) 92–98.
[13] Franklin Associates, Life Cycle Inventory of Three Single-serving Soft Drink Containers. Prairie Village, Kansas, US, 2009.
[14] W. Romão, M.F. Franco, M.I. Bueno, M.A. de Paoli, Distinguishing between virgin and post-consumption bottle-grade poly (ethylene terephthalate) using thermal properties, Polym. Test. (2010). doi:10.1016/j.polymertesting.2010.05.009.
[15] HunterLab, Hunter L, a, b color scale. 2008: 8(9): 1–4.
[16] Y.M. Boiko, G. Guerin, V. Marikhin, R.E. Prud'homme, Healing of interfaces of amorphous and semi-crystalline poly(ethylene terephthalate) in the vicinity of the glass transition temperature, Polym 42 (21) (2001) 8695–8702.
[17] ASTM F1249, Standard Test Method for Water Vapor Transmission Rate Through Plastic Film and Sheeting Using a Modulated Infrared Sensor (2006).
[18] ASTM F3985, Standard Test Method for Oxygen Gas Transmission Rate Through Plastic Film and Sheeting Using a Coulometric Sensor (2005).
[19] R. Hariharan, A. Pinkus, Useful NMR solvent mixture for polyesters: trifluoroacetic acid-d/chloroform-d, Polym. Bull. 30 (1) (1993) 91–95.
[20] ASTM D455, Standard Test Method for Kinematic Viscosity of Transparent and Opaque Liquids (And Calculation of Dynamic Viscosity) (2006).
[21] ASTM D446, Standard Specifications and Operating Instructions for Glass Capillary Kinematic Viscometers (2007).
[22] N. Torres, J. Robin, B. Boutevin, Study of thermal and mechanical properties of virgin and recycled poly (ethylene terephthalate) before and after injection molding, Eur. Polym. J. 36 (10) (2000) 2075–2080.
[23] D.J. Beal, Information Criteria Methods in SAS for Multiple Linear Regression Models. SESUG P, 2007, SA05.
[24] M. Kutner, C. Nachtsheim, J. Neter, W. Li, Applied Linear Statistical Models. McGraw-Hill/Irwin, New York, 2005.
[25] C. Hurvich, C. Tsai, Regression and time series model selection in small samples, Biometrika 76 (2) (1989) 297–307.
[26] J. McDonald, R. Moffitt, The uses of Tobit analysis, Rev. Econ. Stat. 62 (2) (1980) 318–321.
[27] J.L. Koening, Spectroscopy of Polymers. Elsevier Science, New York, 1999.
[28] J. Robinson, E. Frame, G. Frame, Undergraduate Instrumental Analysis. CRC Press, New York, 2005.
[29] D. James, L. Packer, Effect of reaction time on poly (ethylene terephthalate) properties, Ind. Eng. Chem. Res. 34 (11) (1995) 4049–4057.
[30] D. Bikiaris, G. Karayannidis, Effect of carboxylic end groups on thermooxidative stability of PET and PBT, Polym. Degrad. Stabil. 63 (2) (1999) 213–218.
[31] H. Kricheldorf, M. Droscher, W. Hull, 1 H-NMR sequence analysis of poly (ethylene terephthalates) containing various additional diols, Polym. Bull. 4 (9) (1981) 547–554.
[32] J. Brandrup, M. Bittner, Recycling and Recovery of Plastics. Hanser Verlag, Cincinnati, 1996.
[33] D. Belsley, E. Kuh, R. Welsch, Regression Diagnostics: Identifying Influential Data and Sources of Collinearity. Wiley-IEEE, Hoboken, 2004.